

# The maximum contribution to reionization from metal-free stars

J. M. Rozas<sup>1</sup>, J. Miralda-Escudé<sup>2,3</sup> and E. Salvador-Solé<sup>1,4</sup>

## ABSTRACT

We estimate the maximum contribution to reionization from the first generation of massive stars, with zero metallicity, under the assumption that one of these stars forms with a fixed mass in every collapsed halo in which metal-free gas is able to cool. We assume that any halo that has already had stars previously formed in one of their halo progenitors will form only stars with metals, which are assigned an emissivity of ionizing radiation equal to that determined at  $z = 4$  from the measured intensity of the ionizing background. We examine the impact of molecular hydrogen photodissociation (which tends to reduce cooling when a photodissociating background is produced by the first stars) and X-ray photoheating (which heats the atomic medium, raising the entropy of the gas before it collapses into halos). We find that in the CDMA model supported by present observations, and even assuming no negative feedbacks for the formation of metal-free stars, a reionized mass fraction of 50% is not reached until redshift  $z \sim 12$ . The combination of ordinary metal-enriched stars and early metal-free stars can yield a CMB optical depth to electron scattering of at most 0.13. The contribution of metal-free stars to the present Cosmic Infrared Background is negligibly small.

*Subject headings:* cosmology: theory — diffuse radiation — intergalactic medium — galaxies: formation

## 1. Introduction

In the last few years, our understanding of the reionization history of the universe has greatly improved thanks to the detection of quasars at increasingly high redshift (e.g., Becker

---

<sup>1</sup>Departament d'Astronomia i Meteorologia, Universitat de Barcelona, Martí i Franqués 1, 08028 Barcelona, Spain; [jrozas,eduard]@am.ub.es

<sup>2</sup>Department of Astronomy, Ohio State University, 140 West 18th Avenue, Columbus, OH 43210

<sup>3</sup>Institut d'Estudis Espacials de Catalunya/ICREA; miralda@ieec.uab.es

<sup>4</sup>CER on Astrophysics, Particle Physics and Cosmology, Universitat de Barcelona, Martí i Franqués 1, 08028 Barcelona, Spain

et al. 2001; Fan et al. 2002; Hu et al. 2002; White et al. 2003) and the new data on the Cosmic Microwave Background (CMB) radiation from WMAP (Bennet et al. 2003). Observations from high redshift quasars indicate a fast increase of the intensity of the ionizing background with cosmic time occurring at  $z \simeq 6$ , probably signalling the end of reionization (Fan et al. 2002), or the epoch when the low-density intergalactic medium (hereafter, IGM) became fully ionized. Reionization is expected to have occurred over an extended period of time, during which sources gradually reionized every atom in the IGM (e.g., Gnedin 2000). Indeed, the detection of Ly $\alpha$  emission from sources at  $z > 6$  (Hu et al. 2002; Kodaira et al. 2003; Cuby et al. 2003; Kneib et al. 2004; Rhoads et al. 2004) that are not highly luminous to have produced large H $\text{II}$  regions around them implies that the IGM could not be fully neutral at the redshift of these sources, otherwise such photons would have been scattered out of the line of sight (Miralda-Escudé & Rees 1998; Madau & Rees 2000).

Another important probe to the epoch of reionization is the optical depth to electron scattering of CMB photons,  $\tau_e$ . The first measurement of  $\tau_e$  was reported by the *Wilkinson Microwave Anisotropy Probe* mission; although its value is still rather uncertain (Kogut et al. 2003; Spergel et al. 2003), the measurement favored an early start to reionization, such that the fractional ionization of the IGM would have reached 50% at  $z \sim 15$ . It is worth noting that this does not by itself contradict the appearance of the Gunn-Peterson trough (which marks the end of reionization) at  $z \simeq 6$ , because reionization may advance gradually over a long period of time. However, an early start of reionization presents a problem in the Cold Dark Matter model of structure formation, in which only a small fraction of matter has collapsed into halos that can form stars at  $z > 15$ , and therefore one needs to assume a very high rate of emission of ionizing photons from this first generation of stars (e.g., Haiman & Holder 2003; Chiu, Fan, & Ostriker 2003; Onken & Miralda-Escudé 2004). One possibility is that the first collapsed halos in which gas was able to cool were efficient in driving gas to accrete onto central black holes that were formed by the core collapse of the first massive stars. However, as argued by Dijkstra et al. (2004a), any such population of high- $z$  Active Galactic Nuclei (AGN) would likely contribute a smooth component to the present X-ray background at energies near  $\sim 1$  keV that may be higher than is allowed by observational constraints (although significant calibration uncertainties of the X-ray background intensity remain which could increase the upper limit on the fraction of the X-ray background in a smooth component). The other possibility is that the first massive stars, which were metal-free and highly efficient at producing ionizing photons, were responsible for an early reionization (Oh et al. 2001, Yoshida et al. 2003, Sokasian et al. 2004).

Much work has been done to characterize the properties of these metal-free stars (Abel et al. 1998, 2002; Bromm, Coppi, & Larson 1999, 2002; Oh et al. 2001). The formation of the first stars was governed by molecular hydrogen radiative cooling, which becomes effective

at gas temperatures above  $\sim 1000$  K (Yoshida et al. 2003). This virial temperature is first reached in halos of total mass  $\sim 10^6 M_{\odot}$ , which start becoming substantially abundant at  $z \approx 20$ . Metal-free stars have higher effective surface temperatures than their metal-rich counterparts during their main-sequence phase. In addition, they are nearly fully convective and can burn most of their hydrogen content during their main-sequence lifetime. This makes them highly efficient as producers of ionizing radiation (emitting  $\approx 10^5$  ionizing photons per baryon; Schaerer 2002), most of which can escape into the IGM due to the small amount of gas in the host halos.

Despite these advantages of metal-free stars as sources of ionizing radiation, the idea that these stars may have been responsible for an early reionization faces a number of difficulties. First, it is unlikely that many massive stars might form simultaneously in the first halos where star formation took place, which have low velocity dispersion and can therefore easily lose their gas after it is heated by photoionization and supernova explosions. Numerical simulations suggest that one central massive star will initially form, with a mass of  $\sim 200 M_{\odot}$  (e.g., Abel et al. 2002; Bromm et al. 2002), containing a fraction of only  $\sim 10^{-3}$  of the baryonic mass of the halo from which it formed. The ionization and the supernova explosion resulting from this star can then eject the rest of the gas from the halo (Bromm, Yoshida, & Hernquist 2003; Whalen, Abel, & Norman 2004, Kitayama et al. 2004), yielding a very low efficiency to form stars. Later, when the gas falls back into a halo with a total mass increased by the merging process, it will already be enriched by metals and will form the next generation of stars with properties that are presumably similar to present stellar populations in normal galaxies. If the metal-free star releases about  $\sim 100 M_{\odot}$  of metals, a total mass of  $10^7 M_{\odot}$  of baryons may be polluted to a metallicity of  $10^{-3.5} M_{\odot}$ , above which cooling is already modified by the presence of metals, while the emission properties of massive stars are also modified for even lower metallicities. In cases where a metal-free star collapses into a black hole releasing no metals, any cold gas reaching the halo center at a later time will also not form another metal-free star because the black hole will be in the center.

The second difficulty is that the radiation emitted by these first stars can act as a negative feedback mechanism to slow down the formation of other metal-free stars in new collapsed halos with pristine gas. A widely studied effect is photodissociation of molecular hydrogen (Haiman, Abel, & Rees 2000). Another feedback effect is the heating of the IGM by X-rays emitted by supernovae or by the metal-free main-sequence stars themselves (Oh & Haiman 2003), which raises the entropy of gas accreting into halos, resulting in a more stringent requirement for the gas to cool. This effect has not been so widely studied as the molecular photodissociation one, but as we shall see below it may be even more important.

The aim of this paper is to determine the maximum possible contribution to reionization

from zero metallicity stars, under the assumption that only one such star forms in each halo, with a fixed stellar mass. Special attention will be paid to the way that the radiative feedback mechanisms of photodissociation and X-ray heating limit the formation rate of these metal-free stars. We shall use a semianalytic model based on merger trees (similar to the approach of, e.g., Haiman et al. 2000 and Wise & Abel 2005), including a new ingredient to compute the halo age distribution and derive the fraction of halos that contain a metal-free main-sequence star at any given time.

The paper is organized as follows. In § 2, we present our method to calculate the formation rate of metal-free stars, the photodissociating and X-ray background they create, and how these radiation backgrounds affect the formation rate by altering the entropy profile in collapsed halos and the molecular hydrogen abundance. The results are presented in § 3, showing how each of the two feedback effects we consider impact the rate at which metal-free stars can form and their contribution to reionization. A discussion of these results follows in § 4.

## 2. Method

Our central assumption in this paper is that when a halo that contains metal-free gas (i.e., a halo for which no star has previously formed in any of its merger-tree progenitors) collapses, a single massive star forms at the halo center after a cooling time. The mass of this star is assumed to be constant for all halos with metal-free gas. As explained in detail later (§ 2.4), the star forms in our model if the cooling time of the gas at the center of the halo is shorter than the lifetime of the halo. We develop an algorithm to define the lifetime of halos from the merger tree framework based on the extended Press-Schechter model, which is fully described in the appendix. The cooling time depends on the central gas density and temperature, which depends at the same time on the initial entropy of the gas prior to the collapse of the halo (e.g., Oh & Haiman 2003). We compute the initial central gas density (prior to the onset of cooling) in halos at each redshift self-consistently, assuming hydrostatic equilibrium in a halo with the Navarro, Frenk, & White (1997) density profile for the dark matter (hereafter, NFW). We calculate the ionizing radiation emitted by the metal-free stars to infer the history of reionization (taking into account an escape fraction of ionizing photons from halos determined by recombinations in the halo gas), as well as the feedback effects of X-ray heating (and consequent entropy raise of the atomic medium, which affects the gas density profiles in halos) and molecular photodissociation. We also include a component of ionizing radiation from a normal stellar population assumed to form in metal-enriched halos, which have had previous star formation and ionization. This section explains in detail how

all these ingredients are implemented in our model. Our goal will be to find the maximum contribution that these metal-free stars could plausibly make to an early reionization, and how this is limited by the minimal expected feedback effects.

## 2.1. Mass and Age Distribution of Halos

We use the halo mass function of Sheth & Tormen (2002). We assume that a first-generation star forms when the halo age exceeds the cooling time at the halo center. We adopt for this purpose the definition of halo formation time of Lacey & Cole (1993), which is the time when the halo mass was half the present one. The probability distribution of the age of a halo as a function of its mass and redshift is calculated following Lacey & Cole, which we then use to compute the probability that a halo contains a metal-free star as described in the Appendix.

## 2.2. Gas Density Profile

To determine the cooling time at the halo center, we assume the gas is in hydrostatic equilibrium in the halo gravitational potential, and that the dark matter follows a NFW density profile with concentration parameter  $c = 5$ . In reality,  $c$  depends on the halo mass and redshift (Bullock et al. 2001; Eke et al. 2001), but here we approximate it as constant and with the same value used by Oh & Haiman (2003).

Under the assumption of hydrostatic equilibrium, the gas density profile depends on its temperature. Shock-heating of the gas during the collapse heats the gas to a roughly constant temperature, about equal to the halo virial temperature. This results in a final gas density profile similar to the dark matter, although with a small, constant density core, with a size that is determined by the minimum entropy  $K_{min}$  of the gas in the halo. The gas with the lowest entropy is generally the one that is shock-heated to the virial temperature only after reaching a high density, and ends up near the halo center. However, if the gas had already been heated prior to the collapse, acquiring a high initial entropy, the value of  $K_{min}$  may be increased, resulting in a much more extended gas profile and reduced central gas density, and therefore a much longer central cooling time. To take this into account we follow the procedure explained in Oh & Haiman (2003). We define the function  $K$  as

$$K = \frac{T}{n_g^{\gamma-1}} , \quad (1)$$

where  $\gamma$  is the adiabatic index (equal to 5/3 for monatomic gas), and  $T$  and  $n_g$  the gas

temperature and number density. Note that the entropy of a gas is actually the logarithm of  $K$ , although in this paper we refer to the function  $K$  as “entropy” for convenience. The entropy before the collapse is what we call the entropy floor,  $K_{\text{floor}}(t)$ , which we calculate as a function of redshift as described in §2.5.3.

As an example, we show in Figure 1 the gas density profile in a halo with  $M = 5 \times 10^5 \text{ M}_\odot$  formed at different redshifts. The initial entropy is fixed to the primordial value given in Oh & Haiman (2003), determined by early Compton heating by the CMB on the adiabatically cooling gas, with the residual ionized fraction left over from recombination. At  $z < 20$ , the entropy of the IGM is practically constant and the entropy floor decreases in importance with decreasing redshift because of the decreasing gas density, hence the gas density profile becomes steeper at low redshift. We show also the effect of raising the IGM temperature to 100 K at  $z = 10$ , which leads to a large reduction in the central gas density.

### 2.3. Cooling

We define the cooling timescale as the ratio of the internal energy of the gas to the cooling rate per unit of volume,  $L$ :

$$t_{\text{cool}} = \frac{1.5n_g k_{\text{B}} T}{L} , \quad (2)$$

where  $k_{\text{B}}$  is the Boltzmann constant. We include only molecular hydrogen cooling for metal-free gas. In practice, atomic cooling can be neglected because metal-free stars form very rarely in halos with virial temperature above  $\sim 8000$  K in our model. The reason is that these halos usually have some progenitor of lower virial temperature that has already formed a star previously (this will be seen in Fig. 2). In this case, we consider that the gas is already enriched with metals and that the emissivity per unit mass is constant, as described in §2.6.2.

The cooling rate (due to collisional excitation of molecular hydrogen roto-vibrational lines) is  $L_{\text{H}_2} = n_g^2(r) f_{\text{H}_2} \Lambda_{\text{H}_2}$ , where  $f_{\text{H}_2}$  is the molecular fraction. We use the cooling function  $\Lambda_{\text{H}_2}$  of Galli & Palla (1998). The molecular fraction  $f_{\text{H}_2}$  is determined by the continuous formation of molecules in the gas from  $H^-$ , which is at the same time made by the primordial concentration of electrons from the recombination epoch (see Tegmark et al. 1997). We use equation (16) of Tegmark et al., although simplified and modified to consider  $\text{H}_2$  dissociation in the following way:

$$\dot{f}_{\text{H}_2}(r, t) = k_2 n_g f_{e^-}(r, t) - k_{\text{diss}} , \quad (3)$$

where  $k_{\text{diss}}$  is the dissociation rate (which we discuss later in § 2.5.2) and  $f_{e^-}(r, t)$  is the electron fraction, given by equation (14). The constant  $k_2$  determines the formation rate of  $H^-$

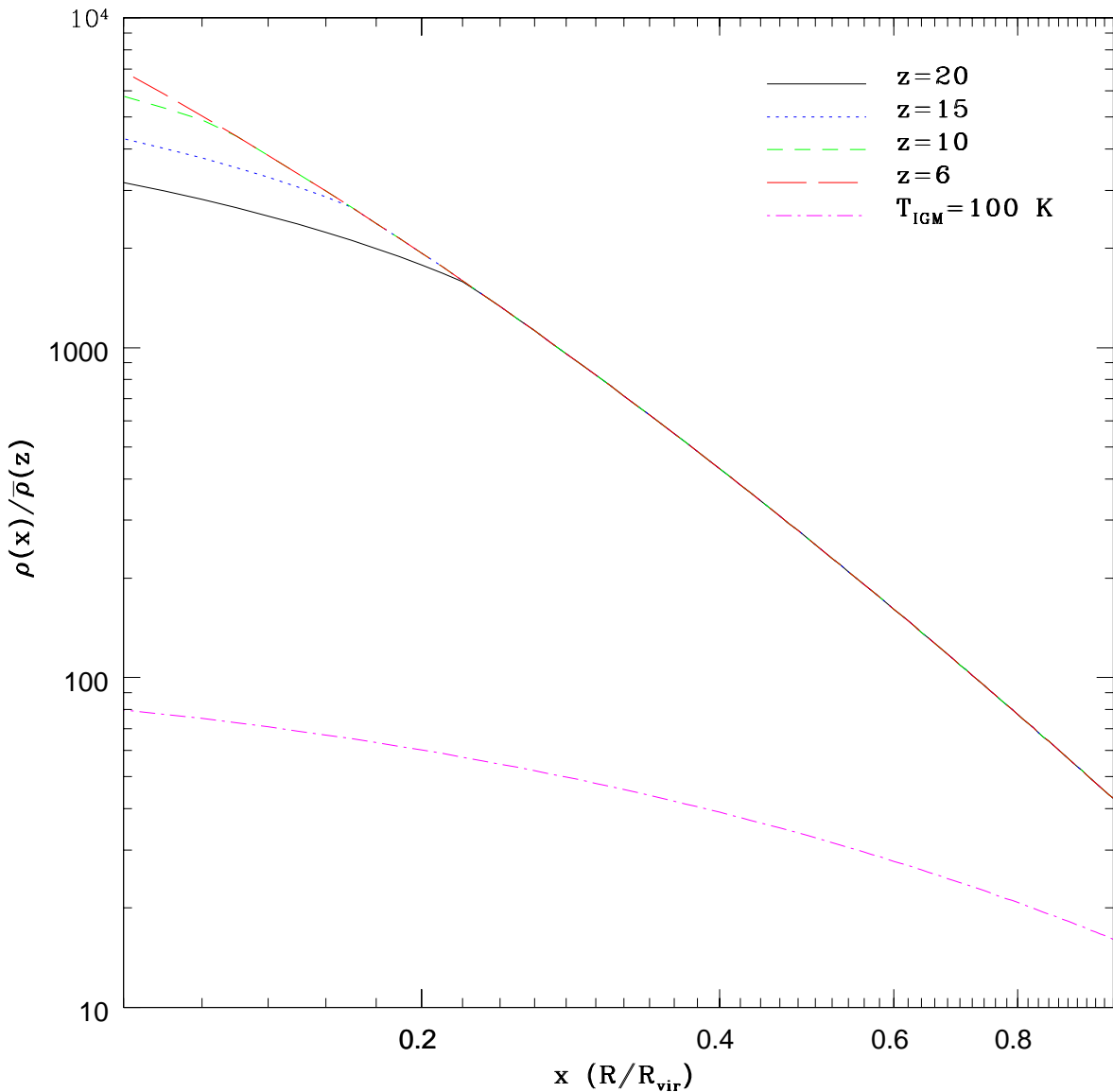


Fig. 1.— Density profiles for a halo of mass  $M = 5 \times 10^5 M_\odot$ . Different lines correspond to halos at different redshift:  $z = 20$  (long dashed line), 15 (short dashed line), 10 (dotted line), and 6 (solid line) with primordial entropy. The last case (dotted dashed line) correspond to redshift 10 but with  $T_{IGM} = 100 K$ .

(which determines the formation rate of molecules), and is given by  $k_2(T) = 1.83 \times 10^{-18} T^{0.88} \text{ cm}^3 \text{ s}^{-1}$ . The initial, primordial value of  $f_{\text{H}_2}$  is taken as  $2 \times 10^{-6}$  (Galli & Palla 1998). Note that the fraction of hydrogen that forms molecules from  $H^-$  within collapsed halos is much larger than this primordial value, and therefore the long-term evolution of the molecular hydrogen fraction does not strongly depend on its initial value.

## 2.4. Star Formation

As mentioned earlier, the main assumption in this work is that only one metal-free star is formed in each halo that collapses from progenitors that have never formed a star previously. The mass of the star,  $M_*$ , is much lower than the baryonic mass of the halo, and is in fact lower than the gas mass in the core of the gas distribution. Consequently, we can evaluate the cooling time at the halo center and consider that the star will form when the age of the halo is equal to this cooling time. The star forms in a halo of mass  $M$  with formation time  $t_f$  at a time  $t_1$  that obeys

$$t_1 = t_f + t_{\text{cool}}(M, t_f) . \quad (4)$$

The star will then live up to a time

$$t_2 = t_1 + t_{mf}(M_*) , \quad (5)$$

where  $t_{mf}(M_*)$  is the main-sequence lifetime of a metal-free star with mass  $M_*$ . The probability that a halo of mass  $M$  at time  $t$  has already formed a star can be evaluated by computing first numerically the formation time  $t_{f1}$  that obeys equation (4) with  $t_1 = t$ , and then calculating the probability  $P_f(M, t, t_f < t_{f1})$  that the halo formation time is earlier than  $t_{f1}$  (see eq. [2.26] of Lacey & Cole 1993). Similarly, the probability that the halo contains a metal-free star on the main-sequence at time  $t$  is evaluated as the probability  $P_f(M, t, t_{f2} < t_f < t_{f1})$ , where  $t_{f2}$  is the solution of  $t_f$  of equation (5) when  $t_2 = t$ .

This condition, however, would be valid only if the halo gas were always metal-free. In reality, if a star had already formed in one of the halo progenitors, the supernova explosion from that star would already have polluted the gas with metals and blown it away. Later on, as the sequence of halo mergers continues, the final halo present at time  $t$  will accrete this gas, but since the gas is metal enriched it will form metal-rich stars. The emission from metal-rich stars will be treated differently in our model, as we describe later in §2.6.2. Here, our main assumption is that the very massive stars we consider that are highly efficient at emitting ionizing radiation are formed only when the gas is totally free of heavy elements.

To take this into account, we evaluate at each time  $t$  the average number of metal-free stars that have formed in a halo of mass  $M$ , as (see the Appendix)

$$N_*(M, t) = \int_0^t dt' \int_0^M dM' N_{LC}(M', t' \rightarrow M, t) \frac{dP_*(M', t')}{dt'}, \quad (6)$$

where  $N_{LC}(M', t' \rightarrow M, t) dM'$  is the number of halos of mass between  $M'$  and  $M' + dM'$  at time  $t'$  that have been incorporated into a halo of mass  $M$  at time  $t$  (see eq. [2.25] in Lacey & Cole 1993), and  $dP_*(M', t')/dt'$  is the probability per unit time that a star forms at  $t'$  in a halo of mass  $M'$ . The way the probability  $dp_*/dt'$  is calculated is described in the Appendix. We then assume that there is a Poisson distribution of the number of stars that have formed within any halo, so that the probability that none has formed is  $\exp(-N_*)$ . Therefore, the probability that a halo of mass  $M$  harbours a main-sequence star at time  $t$  is

$$P_{ms}(M, t) = \int_{t_{f2}}^{t_{f1}} dt' \frac{dP_f(M, t, t')}{dt'} \times e^{-N_*(M, t')}, \quad (7)$$

where  $\frac{dP_f(M, t, t_f)}{dt_f}$  is the differential probability that a halo at time  $t$  was formed at time  $t_f$  and is given by equation (2.19) in Lacey & Cole (1994). In practice, the lifetime of the main-sequence star ( $\sim 3 \times 10^6$  years) is short enough that the above integral can be approximated as

$$P_{ms}(M, t) \simeq \frac{dP_f(M, t, t_{f1})}{dt_f} t_{mf}(M_*) \times e^{-N_*(M, t_{f1})}. \quad (8)$$

Figure 2 shows the probability that a halo with mass  $M$  harbours a metal-free main-sequence star. Different plots correspond to different redshifts ( $z = 20, 15, 10$ , and  $6$ ), and different lines to different models that will be described later. The model A1 corresponds to no feedback effects on the formation of metal-free stars, and the other models incorporate feedback effects that are described in §2.5. The probability to contain a star tends to peak at halo masses of several times  $10^5 M_\odot$ . At lower masses the molecular cooling rate is too slow and stars have not yet formed, while in halos of higher mass a metal-free star has typically already formed in one of their lower-mass progenitors (i.e., the second term in eq. [8] is very small).

As a byproduct, we can also calculate the global formation rate of metal-free stars (see the Appendix) as

$$\dot{N}_*(t) = \int_0^\infty dM N_h(M, t) \frac{dP_*(M, t)}{dt}. \quad (9)$$

where  $\dot{N}_*(t)$  is the metal-free star formation rate and  $N_h(M, t)$  is the Sheth-Tormen halo mass function. This last formula is useful to calculate the preheating due to X-rays (see section 2.5.3).

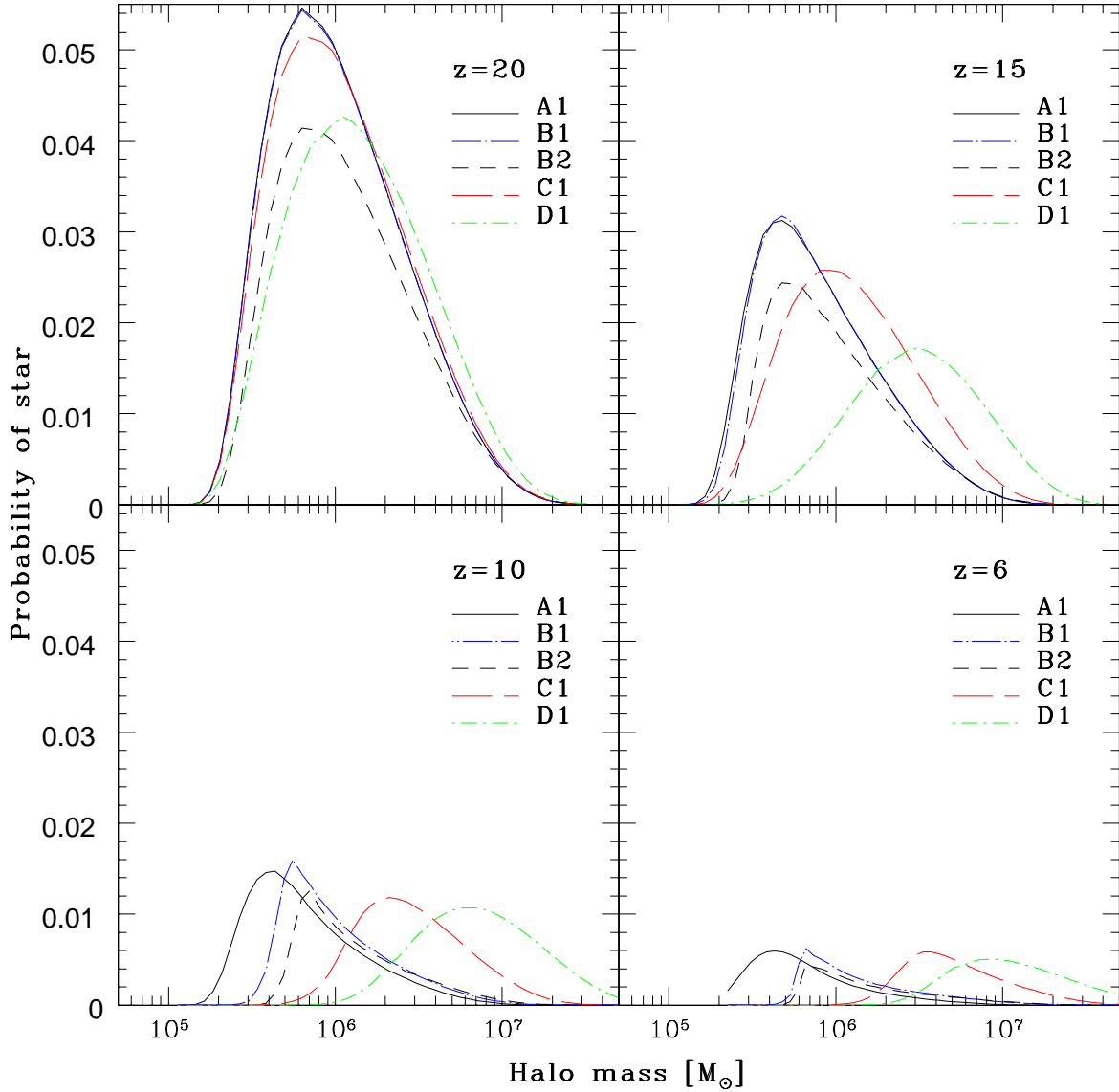


Fig. 2.— Probability that a hydrogen-burning metal-free star is present in a halo at a certain redshift as a function of halo mass. The different cases are those referred in Table 2

## 2.5. Feedback Effects

We consider three feedback processes that affect metal-free star formation. The first is halo photoevaporation due to the ionizing background (section § 2.5.1). The second, photodissociation of molecules due to a soft ultraviolet background (section § 2.5.2). Finally, the third is reheating of the IGM caused by X-rays (section § 2.5.3).

### 2.5.1. Halo Ionization

The ionizing background reheats the gas in halos and causes a large increase in the entropy floor. Gas trapped in minihalos escapes (e.g., Shapiro et al. 2004), quenching star formation. Cooling and star formation in reionized regions can only occur in halos that are massive enough for the gas to undergo dissipation by atomic cooling. We neglect any possible formation of metal-free stars in these halos. In practice, once these halos collapse they should almost always have a progenitor that already formed a metal-free star in the past, because the number of halo progenitors increases with halo mass; moreover, even if one metal-free star may form in one of these more massive halos cooling mainly by atomic processes, their contribution to the total number of metal-free stars formed should be negligible because the abundance of high-mass halos is greatly reduced compared to halos of low mass. We therefore neglect any possible formation of metal-free stars in reionized regions. To take this into account, equation (8) is multiplied by a factor  $1 - f_{\text{ion}}(t)$ , equal to the fraction of the IGM that is neutral at every redshift. The calculation of the ionized fraction of the IGM as a function of time using the global rate of star formation that we compute is described below in §2.6. Actually, the factor  $1 - f_{\text{ion}}$  represents a lower limit to the suppression of the star formation by reionization, because in practice halos are correlated, or biased relative to the mass, so that more halos should be present in the reionized regions where other high-mass halos have already formed.

### 2.5.2. Molecular Photodissociation

$\text{H}_2$  is easily photodissociated by soft ultra-violet photons (Haiman et al. 2000). The rate at which dissociation is produced can be approximated by (Abel et al. 1997)

$$k_{\text{diss}} = 1.38 \times 10^{-12} J_{21}(h\nu = 12.87\text{eV}) F_{\text{shield}} \text{s}^{-1}, \quad (10)$$

being  $J_{21}(h\nu)$  the flux at frequency  $\nu$  in units of  $10^{-21} \text{ergs}^{-1} \text{cm}^{-2} \text{Hz}^{-1} \text{str}^{-1}$  and  $F_{\text{shield}}$  the self-shielding factor given by Draine & Bertoldi (1996).

The mean free path of dissociating photons in the IGM is typically larger than the mean distance between minihalos. Therefore, this flux can be approximated as homogeneous and isotropic. To calculate this background we apply equation (7) of Haiman et al. (2000). The emissivity of dissociating photons ( $j_\nu$  in their formula) is computed similarly to that of ionizing ones (see §2.6.1), although we take into account only the emission by the metal-free stars. Emission from the metal-rich stars has a small effect at the high redshifts of interest, which we have neglected.

### 2.5.3. Reheating of the IGM by X-rays

As proposed by Oh & Haiman (2003), soft X-ray photons raise the entropy floor, greatly reducing cooling and star formation in low-mass halos. X-rays can have a long mean free path through the atomic IGM and can therefore heat this medium in an approximately uniform way, whereas the more abundant ultraviolet ionizing photons heat the medium only near the boundaries of HII regions. The mean free path in the atomic IGM is roughly

$$l_\nu(z) = \frac{42500}{(1+z)^3} \left( \frac{h\nu}{1\text{kev}} \right)^3 \text{Mpc}. \quad (11)$$

When this mean free path is in the range that goes from the mean distance between neighboring halos containing first-generation stars (which is about  $\sim 100$  kpc at  $z = 15$ ; see Yoshida et al. 2003) to the horizon radius ( $\sim 70$  Mpc at  $z = 15$ ), the photons are effective at heating the atomic IGM. This corresponds to a range of frequencies from 200 eV to 2 keV, or the soft X-ray band.

Soft X-ray photons can be produced by metal-free stars during two phases. First, these stars have a high enough effective temperature during the main sequence lifetime to emit substantially in soft X-rays (Schaerer 2002). Second, X-rays can be emitted by the hot gas in a supernova remnant after the death of the star. For simplicity we consider that all the emission is produced at the end of the metal-free star lifetime (a good approximation because of the short lifetime). Therefore, the rate of increase of the entropy floor is

$$\dot{K}_{\text{floor}}(t) = \frac{\dot{T}_{\text{X}}(t)}{n_g^{2/3}(t)} = \frac{2\dot{E}_{\text{reh}}(t)}{3k_{\text{B}}n_g^{2/3}(t)}, \quad (12)$$

where  $\dot{E}_{\text{reh}}(t)$  is the rate of energy increase per particle,

$$\dot{E}_{\text{reh}}(t) = \dot{N}_{\text{SN}}(t)E_{\text{X}}/n_g, \quad (13)$$

and  $\dot{N}_{\text{SN}}(t)$  is the rate of SNe per unit of volume, equal to the star formation rate  $\dot{N}_\star$  (eq. [9]) at the time  $t - t_{mf}(M_\star)$ . The constant  $E_{\text{X}}$  is the total energy per star that is used to reheat

the medium. Note that this is not the same as the total energy radiated in X-rays by the star since some of that energy goes into collisional ionizations or emission of recombination photons. We leave the value of  $E_X$  as a free parameter in our model (the range of possible values is discussed in §3.3).

Even though the reheating by X-rays is roughly homogeneous, the increase of the entropy is of course lower in regions of high gas density. To compute the entropy floor for a specific halo with formation at  $t_f$ , we follow the evolution of the gas density during the collapse assuming the spherical top-hat model, and we compute the entropy increase from the previous history of the intensity of the X-ray background generated by metal-free stars. The evolution of  $\dot{N}_{\text{SN}}(t)$  is computed self-consistently with the model from the star formation rate. Heating by X-rays is no longer taken into account after virialization (this would be negligible in any case once the gas has reached a high density).

X-rays have yet another effect: owing to secondary ionizations, they can produce a higher ionized fraction than the residual value after recombination (which is  $3 \times 10^{-4}$ , see Galli & Palla 1998). This increases the formation rate of molecular hydrogen, enhancing the cooling rate (Haiman, Rees, & Loeb 1996). According to Shull & van Steenberg (1985), around 30 % of the total energy in X-rays is used in ionizations when the neutral fraction is high. The rate of ionizations is then found by dividing expression (13) by 13.6 eV (the ionization energy of hydrogen). Considering this effect, the evolution of  $f_{e^-}$  is determined by

$$\dot{f}_{e^-}(t) = -n_g k_1(T) f_{e^-}(t) + 0.3 \dot{E}_{reh}(t) / 13.6 \text{ eV}, \quad (14)$$

where  $k_1(T)$  is the recombination rate, which can be approximated by  $k_1(T) = 1.88 \times 10^{-10} T^{-0.64} \text{ cm}^3 \text{ s}^{-1}$  (Hutchins 1976) and  $n_g$  is the gas number density in the halo center after collapse. Before collapse, the first term is negligible because the density is very low. The initial value of  $f_{e^-}$  is given by the residual ionized fraction after recombination.

To summarize, for each halo mass at a fixed time, stars can form only when the formation time satisfies equation (4). When considering feedback effects, cooling is delayed and therefore halo formation has to take place earlier. Consequently, the probability that a halo hosts a main sequence star in equation (8) decreases, reflecting the feedback effects.

## 2.6. Reionization

To calculate the reionization history of the IGM we must first calculate the emissivity  $\epsilon(t)$  of ionizing photons per IGM baryon. We consider two contributions to the emissivity, one from metal-free stars which we discuss in § 2.6.1, and another from stars with metals,

discussed in § 2.6.2. Finally, we explain the procedure to calculate the reionization history in § 2.6.1.

### 2.6.1. Metal-Free Star UV Emission

Metal-free stars emit a higher quantity of ionizing photons than enriched stars (see Schaerer (2002)). We use here the fitting formula in Table 6 of Schaerer (2002) to compute the ionizing luminosity of each star as a function of its mass,  $N_{\text{ion}}(M_{\star})$ . For the values of  $M_{\star}$  we consider here, this yields  $N_{\text{ion}}(M_{\star} = 100M_{\odot}) = 1.23 \times 10^{50} \text{ s}^{-1}$  and  $N_{\text{ion}}(M_{\star} = 300M_{\odot}) = 4.52 \times 10^{50} \text{ s}^{-1}$ .

In addition, we take into account that some of the stellar photons may be absorbed locally in the halo gas surrounding the star, and only a fraction  $f_{\text{esc}}$  of these photons will be able to escape and ionize the IGM. We use the following simple model to compute  $f_{\text{esc}}$  (see Whalen et al. 2004 for a more complete discussion and several examples of the evolution of the H II regions formed around a metal-free star): we assume that the star is initially surrounded by a distribution of atomic gas following a singular isothermal profile. An H II region grows around the star, and the heated gas acquires a sound speed of  $\sim 10 \text{ km s}^{-1}$  and starts expanding. This speed is typically larger than the halo circular velocity, but still smaller than the speed of the ionization front as long as the escape fraction is not very small and the star is capable of ionizing the halo (the stellar lifetime is  $\sim 3$  million years, which is short compared to the crossing time of the halo at this sound speed). Hence, the ionization front advances supersonically. We use the simple approximation where all the gas moves out by the same distance  $r_{\text{c}}(t) = 10 \text{ km s}^{-1} \times t$ . The gas distribution then has a central hole of radius  $r_{\text{c}}(t)$ , and at  $r > r_{\text{c}}(t)$  the density is

$$n_{\text{ion}}(r, t) = n[r - r_{\text{c}}(t), 0] \frac{[r - r_{\text{c}}(t)]^2}{r^2}, \quad (15)$$

where  $n(r, 0)$  is the initial gas number density profile of the halo. The total rate of recombinations is computed from this density profile assuming the halo gas has been fully ionized by the star, and is subtracted from the photon emission rate of the star.

The escape fraction of ionizing photons as a function of halo mass ( $f_{\text{esc}}(M)$ ) is plotted for different redshifts in Figure 3. We consider two possible masses of metal-free stars,  $100 M_{\odot}$  (left panel) and  $300 M_{\odot}$  (right panel). Naturally, the escape fraction increases with stellar mass and decreases with halo mass, because the number of recombinations in a halo with the gas fully ionized increases with halo mass and does not depend on the luminosity of the ionizing star. These results agree with the numerical simulations of Kitayama et al. (2004), suggesting that our simple model is able to capture the main physics of the problem. The

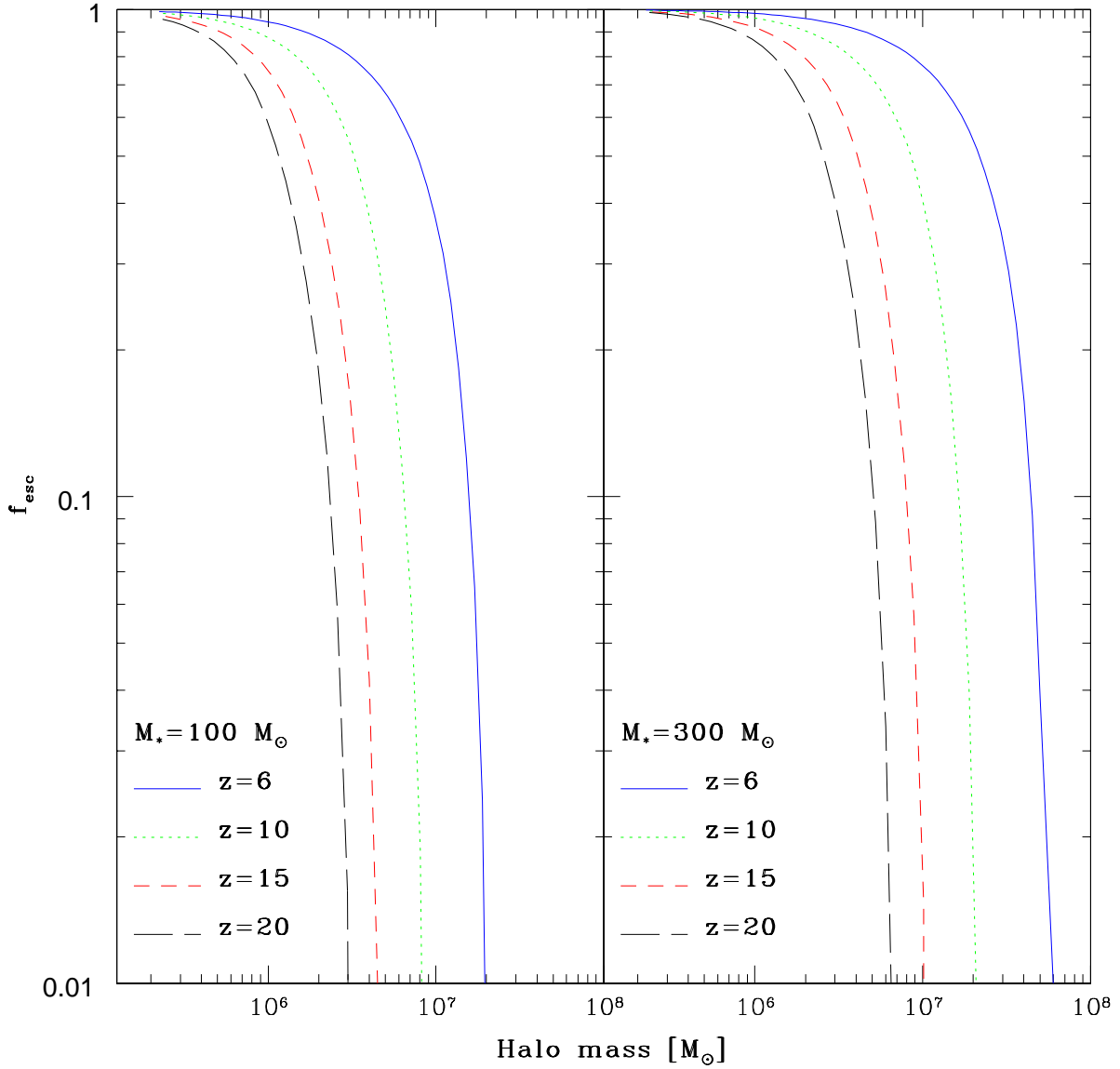


Fig. 3.— Escaping fraction of photons as a function of halo mass for different redshifts, and a metal-free star with the two different masses referred in each plot. Entropy is set as the primordial one.

escape fraction increases when reheating is considered, being more significant in low mass halos, which have their density profiles flattened. Note that there is a halo mass at which the escape fraction falls to zero; for halos above this mass, the single central star is not able to ionize all the halo gas and the H II region reaches a Strömgren radius (the assumption that all the halo gas is ionized is then obviously incorrect, but this affects the calculation of  $f_{esc}$  only when  $f_{esc}$  is already very small in any case).

The global emissivity from metal-free stars,  $\epsilon_{mf}$ , is finally calculated by integrating over all halo masses the number of photons emitted per IGM particle corrected by absorption, i.e.,

$$\epsilon_{mf}(t) = \frac{1}{\bar{n}_g(t)} \int_0^{\infty} dM N_h(M, t) P_{ms}(M, t) f_{esc}(M) N_{\text{ion}}(M_{\star}), \quad (16)$$

where  $\bar{n}_g(t)$  is the baryonic number density of the IGM at  $t$ , and  $P_{ms}(M, t)$  is the probability that a halo harbors a main sequence metal-free star (see eq. 8).

For the emissivity of dissociating photons, we also use equation (16) with  $f_{esc}(M) = 1$ . The emission of dissociating photons from metal-free stars,  $N_{\text{diss}}(M_{\star})$ , is also computed from the fit given in Table 6 in Schaefer (2002) which yields  $N_{\text{diss}}(M_{\star} = 100M_{\odot}) = 1.58 \times 10^{50} \text{ s}^{-1}$  and  $N_{\text{diss}}(M_{\star} = 300M_{\odot}) = 4.74 \times 10^{50} \text{ s}^{-1}$ .

### 2.6.2. Ionizing Emission from Second Generation Stars

After the formation of the first metal-free star in any halo, the surrounding gas is polluted with the metals released by this star. The metal-enriched gas can recombine and fall back into the halo. We assume the metallicity of this infalling gas is then sufficiently high to cool by the usual mechanisms that are prevalent in present galaxies (Bromm et al. 2001). However, halos with metal-enriched gas below a critical virial temperature may still not form stars because the cooling rates are too small (e.g., Dijkstra et al. 2004b), and gas may remain close to  $\sim 10^4$  K in a spherical or thick disk distribution where the gas is unable to cool further and fragment. In this paper, we adopt the simple assumption that in halos where metal-rich star formation takes place, the emissivity per unit baryonic mass is constant at all redshifts. Then, the global emissivity due to enriched stars,  $\epsilon_{mr}(z)$ , is calibrated to the observations of the ionizing background intensity and mean free path of ionizing photons at redshift  $z = 4$  (see Onken & Miralda-Escudé 2004):

$$\epsilon_{mr}(z) = \epsilon_4 \frac{F(z)}{F_4}, \quad (17)$$

where  $\epsilon_4$  is the emissivity at redshift 4 in units of ionising photons per particle and per Hubble time,  $F(z)$  is the fraction of mass in halos where metal-rich star formation takes

place, and  $F_4$  is the same fraction of mass at  $z = 4$ . We assume that halos with circular velocity above 35 km/s are the ones forming stars at  $z = 4$  (as in Onken & Miralda-Escudé 2004; this affects only the normalization of the emissivity), but consider different possibilities for the emissivity at higher redshift, as explained below.

In order to study the effect of varying the emission from normal, metal-rich galaxies, we consider several models listed in Table 1. These models are labeled by a number, and in general any model will be referred to by the letter specifying the feedback processes assumed (see Table 1) and this number. In Models 1 and 2, we compute  $F(z)$  as the fraction of mass in metal-enriched halos with a circular velocity greater than 10 km/s, and in Models 3 to 6 we assume that all halos that have been polluted by metals form enriched stars, with no minimum halo circular velocity. Note that even by assuming a minimum halo circular velocity that is lower than at the calibration redshift  $z = 4$ , we are maximizing the emission at high redshift under the constraint that the emission per unit mass is not greater than in halos at  $z = 4$ . The value of the normalization constant  $\epsilon_4$  is also subject to uncertainties arising from the process by which the intensity of the ionizing background is inferred from modelling the Ly $\alpha$  forest transmitted flux, and the measurement of the photon mean free path from the abundance of Lyman limit systems. We adopt the values  $\epsilon_4 = 7$  for Models 1 to 4 (as in Miralda-Escudé 2003), and twice this value,  $\epsilon_4 = 14$  (which would be favored by the measurement of the ionizing background intensity by Bolton et al. 2005), in Models 5 and 6.

Finally, the emissivity from the metal-free stars is varied by considering all stars to have a mass  $M_\star = 100M_\odot$  in models with odd number, and  $M_\star = 300M_\odot$  in models with even number.

### 2.6.3. Reionization History and Optical Depth

The evolution of the ionized fraction  $f_{\text{ion}}(t)$  is calculated according to

$$\frac{df_{\text{ion}}(t)}{dt} = \epsilon(t) - \bar{n}_g^2(t) k_1 f_{\text{ion}}(t) , \quad (18)$$

where  $\epsilon(t) = \epsilon_{mf}(t) + \epsilon_{mr}(t)$  is the total emissivity of ionizing photons, and  $k_1$  is the recombination rate which we evaluate at  $T = 10^4$  K. The cosmic history of  $f_{\text{ion}}(t)$  then yields the electron scattering optical depth  $\tau_e$ .

### 3. Results

In this section, we present the results on metal-free star formation and the reionization history of the IGM obtained from the approach given in §2. In this model, there are four free parameters: the stellar mass,  $M_*$ , the reheating of IGM per metal-free star,  $E_X$ , and the emissivity of metal-rich stars,  $\epsilon_4$ . In addition, there is some uncertainty in the physical processes governing feedback effects. For this reason, we play with the possibility to switch on or off the effect of photodissociating photons in order to check how important it is. Finally, to compute  $F(z)$  in equation (17) we may consider or not halos with circular velocity  $< 10$  km/s (minihalos) to see whether the value of  $\tau_e$  experiences a big change. The models including all the different possibilities are labelled XY, with X running from A to D and Y running from 1 to 6 (see Tables 1 and 2).

We now present the results on the rate of metal-free star formation and the reionization history of the IGM for the models described in §2. The models and their nomenclature are described in Tables 1 and 2. The model number (1 to 6) refers to properties of the radiation sources: the mass of metal-free stars, and the normalization and low halo mass cutoff for the emission from metal-enriched stars. The model letter (A to D) refers to the presence or absence of the molecular photodissociation and X-ray heating feedback effects. Results are first presented for the case of no feedback effects (Models A, § 3.1), then including molecular photodissociation (Models B, § 3.2), and finally including X-ray photoheating (Models C and D, § 3.3). Then, the reionization histories are reviewed (§ 3.4). All models are run with the following set of cosmological parameters:  $\Omega_m = 0.27$ ,  $\Omega_\Lambda = 0.73$ ,  $\Omega_b = 0.045$ ,  $h_0 = 0.71$ ,  $\sigma_8 = 0.84$  and  $n = 1$ .

#### 3.1. No Feedback Effects

The evolution of the emissivity for Model A1 is shown in Figure 4, both for metal-free and metal-rich stars. Metal-free stars dominate at high redshift, and enriched stars start dominating below  $z \sim 10$ . This behaviour is easily understood. Initially there are only metal-free stars and their contribution grows with time as more halos form. This results in an increasing fraction of halos being polluted with metals, which at some point causes a decline in the rate of new metal-free stars that are formed. The halos collapsing with enriched gas start forming enriched stars which eventually dominate the emissivity. The formation of metal-free stars is also reduced as redshift decreases due to the increased fraction of the IGM that is ionized. In ionized regions, the gas is less able to cool and low-mass halos would continue merging into more massive ones before forming any stars, implying a great reduction in the number of metal-free stars that can be formed. This effect is less important

Table 1. *First column:* Source model number. *Second column:* Emissivity normalization parameter for metal-enriched stars,  $\epsilon_4$ . *Third column:* Contribution of minihalos to metal-enriched stars. *Fourth column:* Mass of metal-free stars.

Source model	$\epsilon_4$	Minihalos	$M_\star [M_\odot]$
1	7	No	100
2	7	No	300
3	7	Yes	100
4	7	Yes	300
5	14	Yes	100
6	14	Yes	300

Table 2. *First column:* Feedback model letter. *Second column:* Presence of a molecular photodissociating background. *Third column:* Energy used to heat the intergalactic medium by soft X-rays per metal-free star.

Feedback model	Photodiss.	$E_X [erg]$
A	No	0
B	Yes	0
C	Yes	$10^{51}$
D	Yes	$10^{52}$

because the IGM ionized fraction remains relatively low at the epoch where most metal-free stars form.

Comparing Models 1 (with metal-free stellar mass of  $M_\star = 100M_\odot$ ) with Models 2 ( $M_\star = 300M_\odot$ ), Figure 4 shows that the emissivity of metal-free stars increases by a factor of 3 as expected at  $z \gtrsim 20$ , but at lower redshift it increases by a smaller factor because the fraction of ionized IGM increases faster for  $M_\star = 300M_\odot$ , reducing the formation of metal free stars to a greater extent than for Models 1. We note here that a high bias in the distribution of metal-free stars relative to the mass could further increase the effect of ionization in suppressing the number of metal-free stars that can be formed.

### 3.2. Effect of Molecular Photodissociation

We now examine how the inclusion of a photodissociating background, computed self-consistently from the star formation history, alters the results. Figure 5 shows the evolution of the photodissociating background intensity in Models B1 and B2. The maximum is reached around  $z \sim 15$  as the effects of increased metal pollution and ionized IGM fraction suppress new metal-free star formation (note that emission from enriched stars is not included in this figure). Figure 4 shows that the maximum of formation rate of metal-free stars occurs at higher redshift when the photodissociating feedback is included, because of the additional suppression of star formation. We also see in Figure 2 how the formation of metal-free stars is shifted to higher mass halos in Models A compared to Models B at  $z \lesssim 15$ , because the negative feedback delays the formation of the stars to a later stage at which halos have grown to a higher mass.

### 3.3. Effect of IGM Reheating by X-rays

We consider two models for the soft X-ray energy produced by a metal-free star that is converted into IGM heat,  $E_X$  (Table 2, Models C and D). During the main-sequence, and at effective surface temperatures near  $\sim 10^5$  K, the fraction of radiative energy emitted above  $200eV$  is  $\sim 0.1\%$  of the total energy output of the star, or  $\sim 10^{51}$  erg. The supernova explosion at the end of the life of a metal-free star can produce as much as  $10^{53}$  erg of kinetic energy for some stellar masses (see, e.g., Bromm et al. 2003), and the fraction of these kinetic energy that is eventually reprocessed into soft X-rays may be  $\sim 0.03$  (Oh & Haiman 2003), of which a fraction of 50% may be converted into IGM heat when the soft X-rays are absorbed in a mostly neutral medium (Shull & van Steenberg 1985). Given the substantial degree of

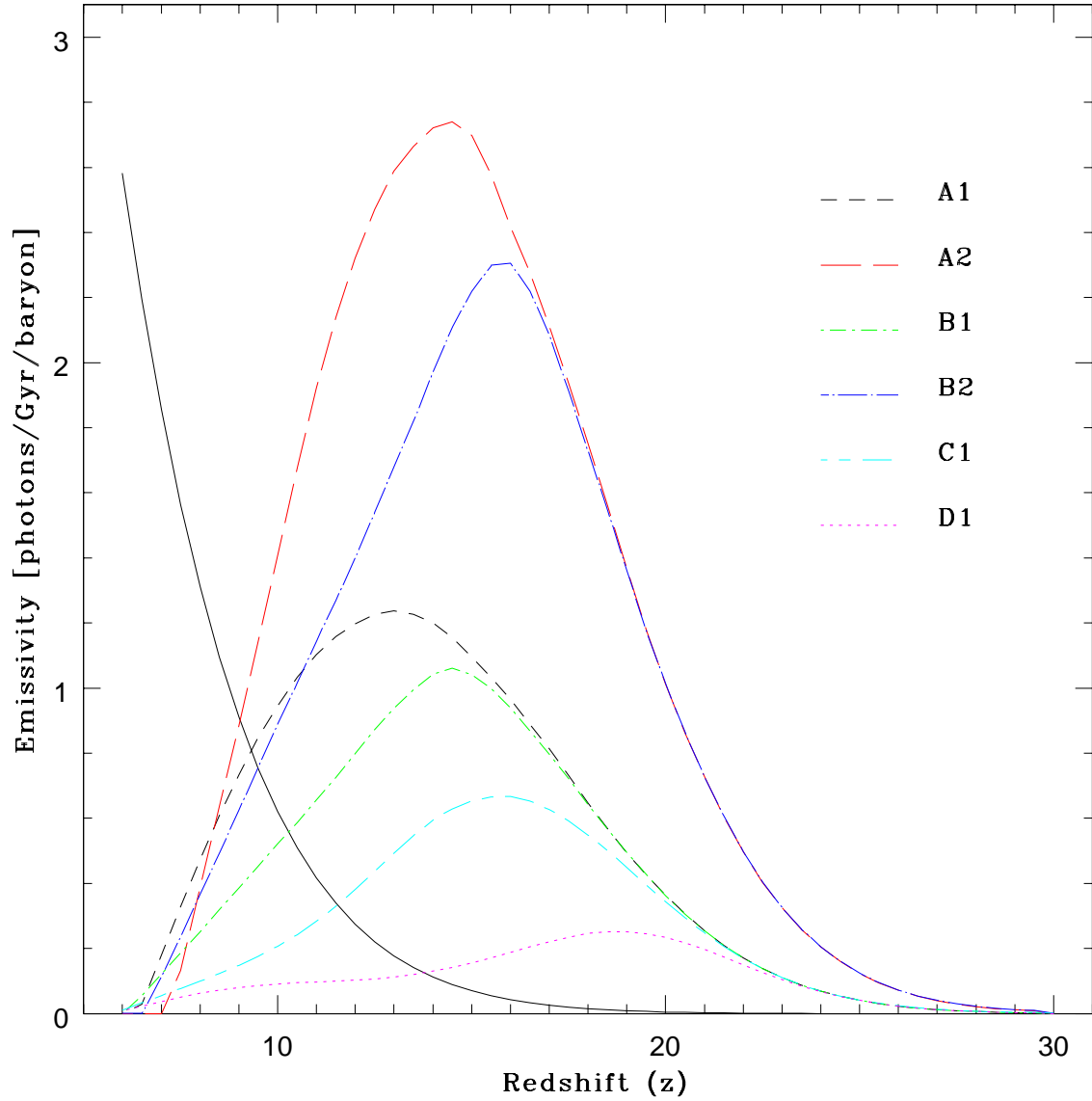


Fig. 4.— Emissivity as a function of redshift from metal-rich (continuous line) and metal-free (dashed lines) stars for different models. The total emissivity is the sum of the two.

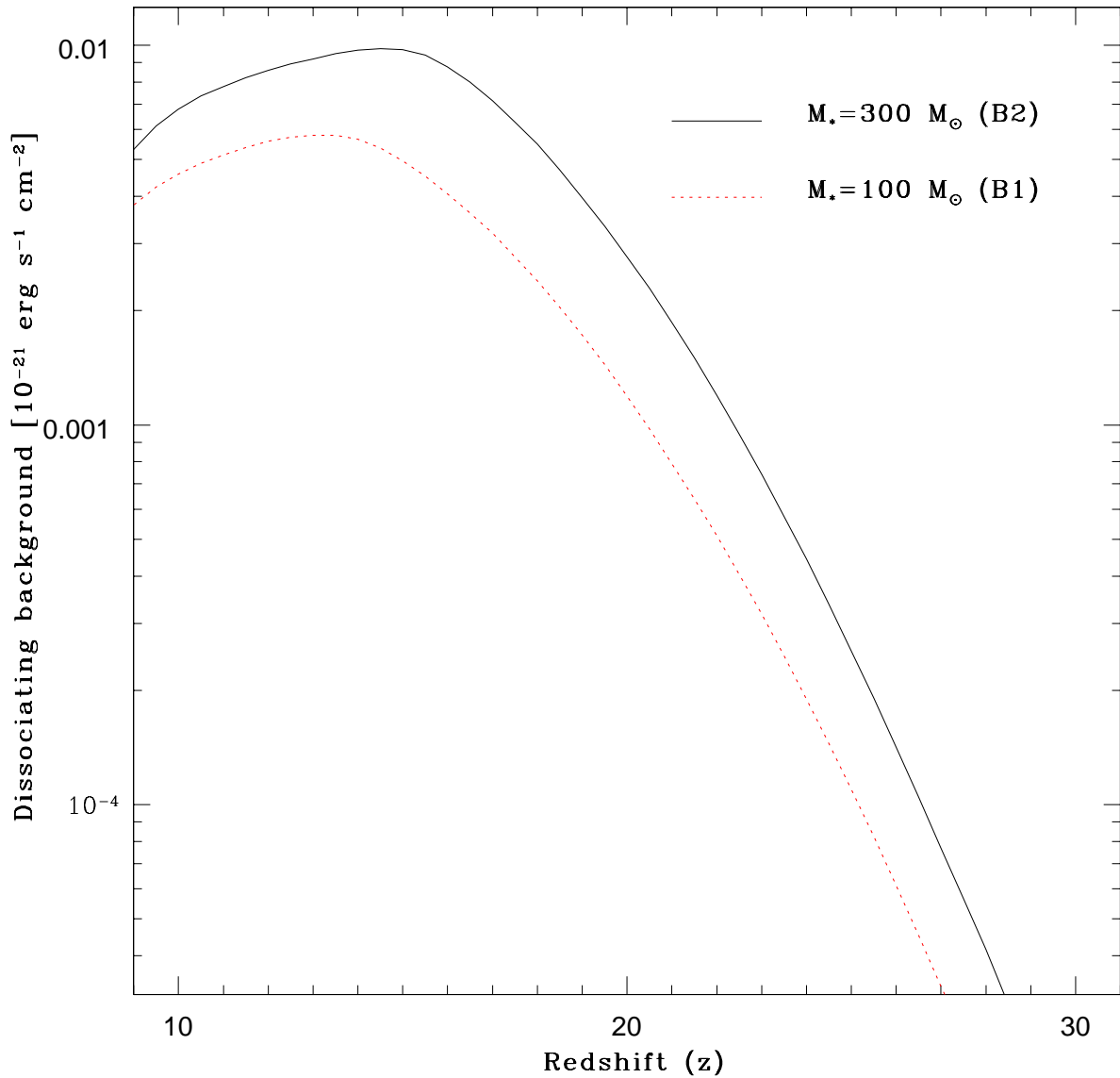


Fig. 5.— Photodissociating flux as a function of redshift for Models B1 and B2 (varying only the metal-free stellar mass)

uncertainty in the soft X-ray energy emitted per star, we consider the two values in Models C and D bracketing our estimate.

The increase in IGM temperature caused by the absorption of soft X-rays is shown in Figure 6 for Models C1 and D1. The onset of formation of metal-free stars causes a rise in temperature of the neutral medium starting at  $z \sim 25$ , and at lower redshift the temperature ceases to increase when the formation of metal-free stars is reduced (in practice there would probably be an important contribution to the X-ray emission from the enriched population, which has been considered here).

The establishment of an entropy floor causes a large reduction of the central density in low mass halos (see Fig. 1), which greatly reduces the cooling rate. This implies that metal-free stars tend to be formed in Models C and D in much more massive halos than in Models A and B: the formation of these stars is suppressed in low-mass halos by the feedback effect, so metal-free stars are not formed until later when a more massive halo has formed from the mergers of several small ones (see Figure 2). As long as our assumption that only one metal-free star forms in each halo continues to hold, the metal-free stars will be much less abundant. This is seen clearly in Figure 4, which shows the large reduction in the emissivity of metal-free stars caused by the soft X-ray heating.

### 3.4. Reionization

Finally, we examine the reionization history and electron scattering optical depth to the CMB of electron scattering in all the models. In Figure 7 we see that, as expected, feedback delays the ionization of the IGM. Reionization always occurs gradually over a relatively wide redshift range. Naturally, models with the highest stellar mass and emission from enriched stars achieve a higher ionized fraction at every redshift, and hence a higher optical depth. Even though the total emissivity history may be double-peaked owing to the presence of the metal-free and the enriched populations of stars (see Fig. 4), there is never a double reionization because the recombination rate is slow enough that the ionized fraction continues to increase when the emission from metal-free stars starts decreasing.

The redshift at which reionization is completed stays in the range of 6–9. This prediction of the redshift of the end of reionization is a natural consequence of the value of the emissivity assumed for the enriched stars that is derived from observations of Ly $\alpha$  absorption systems at  $z \lesssim 5$ , and of assuming that the clumping factor of ionized gas is not much larger than unity (Miralda-Escudé 2003). The exact redshift of the end of reionization predicted by each model is not an independent test of our models, because this redshift can be modified

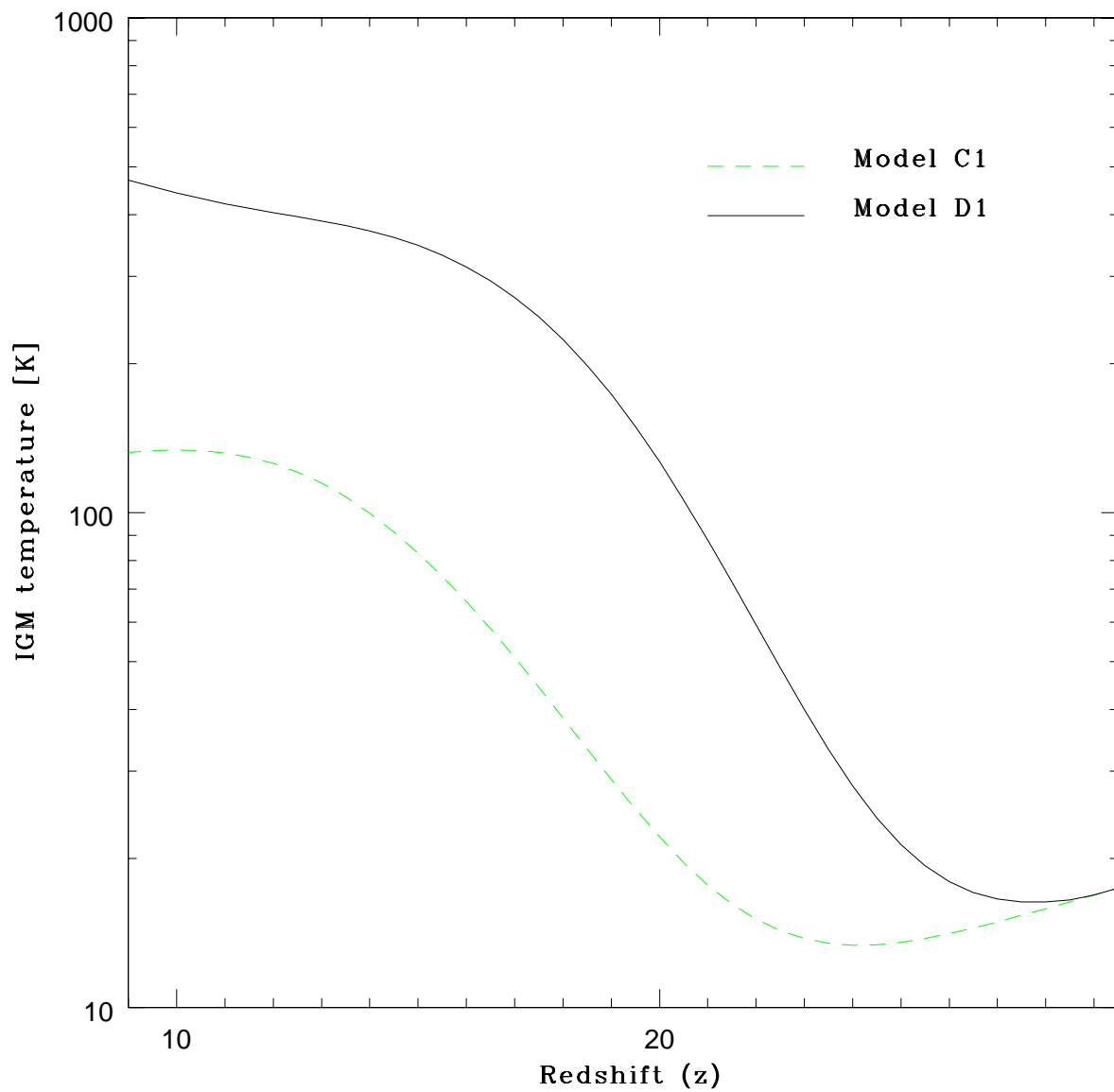


Fig. 6.— IGM temperature including soft X-ray heating.

and adjusted to agree with observations of the Gunn-Peterson trough in the highest redshift quasars (White et al. 2003) by introducing a moderate clumping factor with an adequate dependence on redshift (note that we have assumed a clumping factor equal to one).

The values of the electron scattering optical depth for each model are presented in Table 3. The presence of metal-free stars has an important effect in creating a small ionized fraction at very high redshifts ( $z \sim 20$ ). However, the increase of the optical depth that metal-free stars can cause is modest and, even for  $M_* = 300M_\odot$  and in the absence of any negative feedback effects, they do not increase the optical depth beyond  $\sim 0.12$ . Models D1, D3 and D5 represent cases where the contribution from metal-free stars is minimal (due to the very strong X-ray heating assumed; see Fig. 4). Comparing them with models A2, A4 and A6 where the emission from metal-free stars is maximum, we see that the early ionization caused by metal-free stars can cause only a relatively modest increase of the optical depth, under our central assumption that only one metal-free star is made per halo, and no metal-free stars are made in halos that have already merged with a halo in which star had previously formed.

#### 4. Discussion and Conclusions

We have considered in this paper the maximum emissivity and the contribution to reionization that metal-free stars could make. Our central assumption is that only one metal-free star is made in every halo where pristine gas is able to cool via molecular hydrogen rotovibrational lines. This is a reasonable assumption in view of the simulations that have been made of the formation of the first star and the effects of the subsequent ionizing radiation emitted and supernova explosion: the gas cools hydrostatically towards the center, avoiding fragmentation and forming a central star which can then ionize and heat all the gas in its host halo, and probably expel it in the supernova explosion (e.g., Abel et al. 2002; Bromm et al. 2002, 2003). Once a star has exploded, it pollutes its host halo as well as every larger halo into which its host halo merges in the future. Any halo that has already formed a metal-free star in any of its halo progenitors in the past is assumed to form a metal-enriched population of stars that has an emissivity of ionizing photons similar to the emissivity that is observationally determined at  $z \sim 4$ .

Under this basic assumption, the contribution of the metal-free stars to reionization is relatively modest. Metal-free stars may dominate the emissivity at very high redshifts ( $z \gtrsim 10$ ), but before they can manage to ionize much of the universe, the metal pollution of halos rapidly reduces their formation rate. Moreover, the effects of the ionization itself prevent cooling in the remaining low-mass halos with pristine gas, delaying the formation of

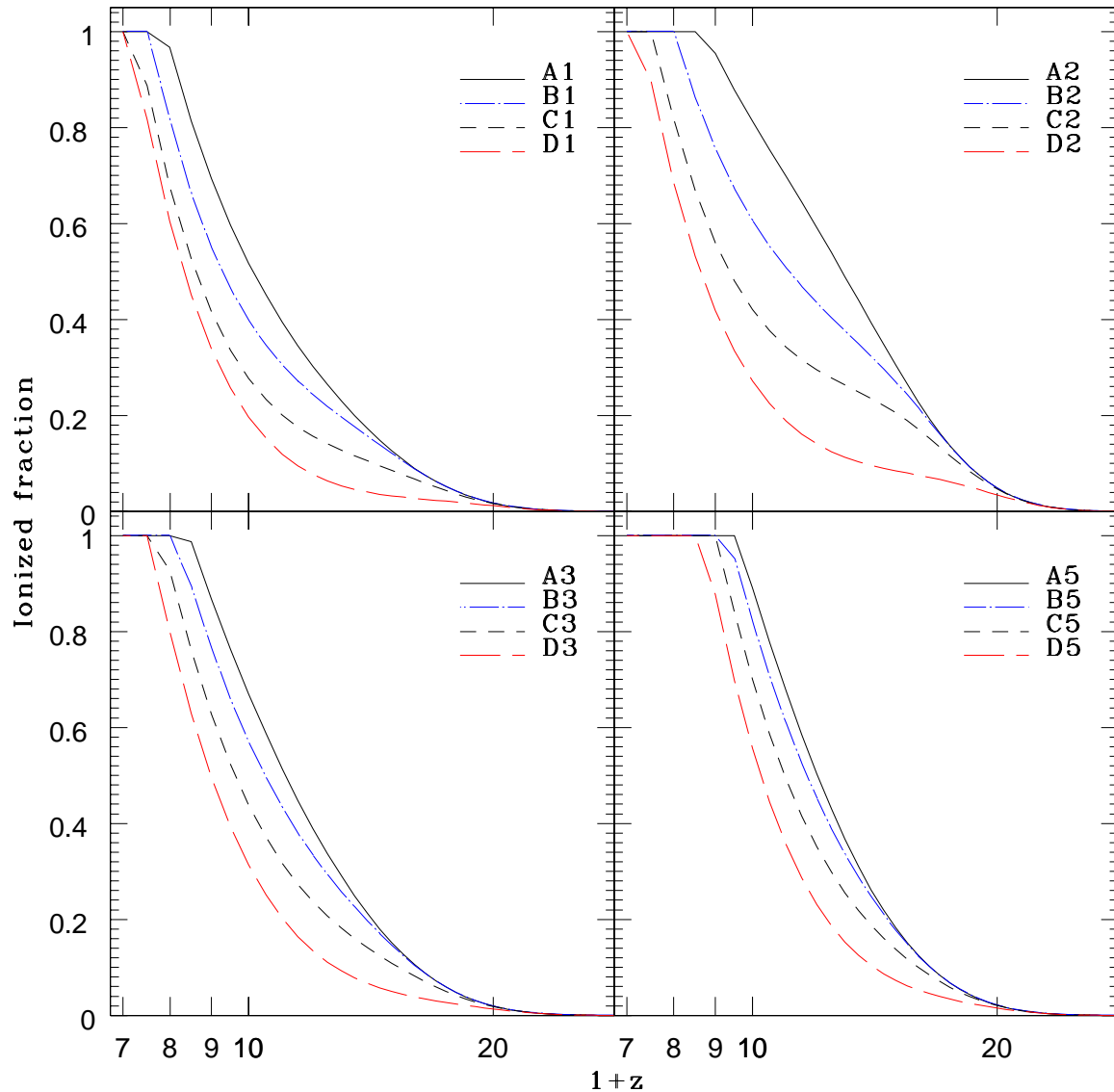


Fig. 7.— Ionized fraction as a function of redshift, for the indicated models.

a central metal-free star to the time of formation of more massive halos that collapse later, and thereby reducing the number of metal-free stars that are formed per unit of mass in the universe. Reionization was likely completed by a population of stars and quasars in galaxies forming from pre-enriched gas.

We have analyzed the effects of molecular photodissociation and of increasing the entropy floor by X-ray heating. These can further reduce the amount of ionizing radiation that is emitted by the population of metal-free stars. In agreement with Oh & Haiman (2003), we have found that the negative feedback induced by X-ray heating can in principle be very large. However, as pointed out by Kuhlen & Madau (2005), this negative feedback might be much less important than suggested by the simple calculation of Oh & Haiman (2003) and the one we have presented here. In our calculation, we consider only the cooling time of the gas at the halo center in the hydrostatic equilibrium configuration obtained at the end, by assuming an increased initial entropy produced by the X-ray heating. In reality, the gas should be able to gradually cool and lose entropy as it collapses in dense regions of halos, and these halos later merge to form the final one where a star is formed. The same X-rays that heat the gas would also increase the ionization, allowing faster molecular cooling as the gas density increases, which might greatly reduce the X-ray negative feedback effect. Nevertheless, our main conclusion is that even without feedback effects the emission from metal-free stars is strongly limited by the metal-pollution and the ionization itself.

Our models are generally in agreement with previous work. The value of  $\tau_e$  we infer is always lower than 0.13, even when we increase the emissivity of the enriched stellar population and we minimize any negative feedback effects on the metal-free population. For a smaller contribution from metal-free stars, values of  $\tau_e$  are closer to 0.10 (see Table 3), in agreement with the results of Ricotti & Ostriker (2004). Our results are also compatible with those of Sokasian et al. (2004), who find that high CMB optical depths to electron scattering can be achieved only when many stars are assumed to be formed within halos that cool by molecular hydrogen. The model M9 of Sokasian et al. is the only one that assumes that only one star is formed per halo, and in this case their results for the maximum optical depth are in good agreement with ours. Similarly, Wise & Abel (2005) can also produce high optical depths only by assuming that many metal-free stars form in each halo with a total mass much larger than in our model.

Naturally, if one is willing to assume a mass for metal-free stars even larger than  $300M_\odot$ , their contribution to the CMB optical depth,  $\tau_e$ , can be further increased, but their total emission increases by a factor smaller than the increase in the mass because of the enhanced negative feedbacks. At the same time, if miniquasars emitting copious amounts of ionizing radiation where produced by the black holes created by the metal-free stars (which could

occur when a halo containing a central clump of cooling gas merges with another halo that has already formed a star and contains a black hole in its center), much more ionizing radiation could be produced, although the X-rays emitted by these mini-quasars might then be in conflict with limits on any unresolved component of the present soft X-ray background (Dijkstra et al. 2004a).

Our work can also be used to estimate the contribution of metal-free stars to the Cosmic Infrared Background, which might include the ultraviolet light of these stars from high redshift. The total number of ionizing photons that are ever emitted by metal-free stars can be computed straightforwardly by integrating the curves shown in Figure 4. The results are shown in Table 4 for each one of our models. Even in the absence of negative feedbacks, and for stellar masses  $M_\star = 300M_\odot$ , metal-free stars do not emit more than  $\sim$  one photon per baryon in the universe. This conclusion is not surprising, since in the absence of many recombinations one does not need a large number of ionizing photons to be emitted per baryon to complete the reionization. Because of the very high effective temperatures of metal-free stars ( $T \sim 10^5$  K), the number of photons emitted in ultraviolet light at wavelengths longer than the Lyman limit is similar. Hence, the contribution of metal-free stars to the present Cosmic Infrared Background is not more than  $\sim$  one photon per baryon under the assumptions we have made.

Recently, Kashlinsky et al. (2005) detected brightness fluctuations in the Cosmic Infrared Background after subtracting all contributions from known galaxies. The measured fluctuations are at a level of  $\sim 0.1nWm^{-2} sr^{-1}$ . This background intensity at a wavelength of  $5\mu m$  corresponds to  $\sim 500$  photons per baryon in the universe; as discussed by Kashlinsky et al. , in order to account for the observed fluctuations the absolute brightness of the infrared background contributed by metal-free stars would have to be as high as  $\sim 1nWm^{-2} sr^{-1}$  (or  $\sim 5000$  photons emitted per baryon), after taking into account the expected high bias in the spatial distribution of these stars. It is clear that very extreme assumptions about the number of metal-free stars that were formed need to be made if the unaccounted fluctuations in the Cosmic Infrared Background are related in any way to these metal-free stars. As discussed by Santos et al. (2002), if metal-free stars are to make an important contribution to the Cosmic Infrared Background, one needs to assume that a large fraction of all the gas in each halo where pristine gas cools by molecular hydrogen (typically more than  $10^5M_\odot$  ) forms metal-free stars, and that most of the radiation from the stars is somehow internally absorbed in the halos in order to prevent an excessively early reionization of the IGM. Both of these requirements are not realistic: once a central star is formed in a  $\sim 10^6M_\odot$  halo, its ionizing radiation will ionize and push all the halo gas out over the short main-sequence lifetime of the star, and the escape fraction of the ionizing photons is high except in rare cases where a single star forms in a very massive halo (see Figure 3). The detected Cosmic

Infrared Background fluctuations have other more likely possible sources, such as an incomplete accounting of the faint-end of the galaxy luminosity function, or a normal population of low-luminosity galaxies with metal-enriched gas and stars at high redshift.

JM acknowledges helpful conversations with Mark Kuhnen, Piero Madau, and Daniel Wang. JM would also like to thank the Institute for Advanced Study for their hospitality, where part of this work was completed. This work was supported in part by the Dirección General de Investigación Científica y Técnica of Spain, under contract AYA2003-07468-C03-01. JMR was supported by a fellowship of the Ministerio de Educación, Cultura y Deporte of Spain.

## REFERENCES

Abel, T., Anninos, P., Zhang, Y., & Norman, M. L. 1997, *New Astronomy*, 2, 181

Abel, T., Bryan, G. L., & Norman, M. L. 2002, *Science*, 295, 93

Becker, R. H., et al. 2001, *AJ*, 122, 2850

Bennett, C. L., et al. 2003, *ApJS*, 148, 1

Bolton, J. S., Haehnelt, M. G., Viel, M., & Springel, V. 2005, *MNRAS*, 357, 1178

Bromm, V., Coppi, P. S., & Larson, R. B. 2002, *ApJ*, 564, 23

Bromm, V., Ferrara, A., Coppi, P. S., & Larson, R. B. 2001, *MNRAS*, 328, 969

Bromm, V., Yoshida, N., & Hernquist, L. 2003, *ApJ*, 596, L135

Bullock, J. S., Kolatt, T. S., Sigad, Y., Somerville, R. S., Kravtsov, A. V., Klypin, A. A., Primack, J. R., & Dekel, A. 2001, *MNRAS*, 321, 559

Chiu, W. A., Fan, X., & Ostriker, J. P. 2003, *ApJ*, 599, 759

Cuby, J.-G., Le Fèvre, O., McCracken, H., Cuillandre, J.-C., Magnier, E., & Meneux, B. 2003, *A&A*, 405, L19

Dijkstra, M., Haiman, Z., & Loeb, A. 2004a, *ApJ*, 613, 646

Dijkstra, M., Haiman, Z., Rees, M. J., & Weinberg, D. H. 2004b, *ApJ*, 601, 666

Draine, B. T. & Bertoldi, F. 1996, *ApJ*, 468, 269

Eke, V. R., Navarro, J. F., & Steinmetz, M. 2001, *ApJ*, 554, 114

Fan, X., Narayanan, V. K., Strauss, M. A., White, R. L., Becker, R. H., Pentericci, L., & Rix, H. 2002, *AJ*, 123, 1247

Galli, D. & Palla, F. 1998, *A&A*, 335, 403

Gnedin, N. Y. 2000, *ApJ*, 535, 530

Haiman, Z., Abel, T., & Rees, M. J. 2000, *ApJ*, 534, 11

Haiman, Z., & Holder, G. P. 2003, *ApJ*, 595, 1

Haiman, Z., Rees, M. J., & Loeb, A. 1996, *ApJ*, 467, 522

Hu, E. M., Cowie, L. L., McMahon, R. G., Capak, P., Iwamuro, F., Kneib, J.-P., Maihara, T., & Motohara, K. 2002, *ApJ*, 568, L75

Hutchins, J. B. 1976, *ApJ*, 205, 103

Kashlinsky, A., Arendt, R. G., Mather, J., & Moseley, S. H. 2005, *Nature*, 438, 45

Kitayama, T., Yoshida, N., Susa, H., & Umemura, M. 2004, *ApJ*, 613, 631

Kneib, J., Ellis, R. S., Santos, M. R., & Richard, J. 2004, *ApJ*, 607, 697

Kodaira, K., et al. 2003, *PASJ*, 55, L17

Kogut, A., et al. 2003, *ApJS*, 148, 161

Kuhlen, M., & Madau, P. 2005, *MNRAS*, 860

Lacey, C. & Cole, S. 1993, *MNRAS*, 262, 627

Lacey, C. & Cole, S. 1993, *MNRAS*, 271, 676

Madau, P., & Rees, M. J. 2000, *ApJ*, 542, L69

Miralda-Escudé, J. 2003, *ApJ*, 597, 66

Miralda-Escude, J., & Rees, M. J. 1998, *ApJ*, 497, 21

Navarro, J. F., Frenk, C. S., & White, S. D. M. 1997, *ApJ*, 490, 493

Oh, S. P. & Haiman, Z. 2003, *MNRAS*, 346, 456

Onken, C. A. & Miralda-Escudé, J. 2004, *ApJ*, 610, 1

Oh, S. P., Nollett, K. M., Madau, P., & Wasserburg, G. J. 2001, ApJ, 562, L10

Raig, A., González-Casado, G., & Salvador-Solé, E. 2001, MNRAS, 327, 939

Rhoads, J. E., et al. 2004, ApJ, 611, 59

Ricotti, M., & Ostriker, J. P. 2004, MNRAS, 350, 539

Santos, M. R., Bromm, V., & Kamionkowski, M. 2002, MNRAS, 336, 1082

Schaerer, D. 2002, A&A, 382, 28

Shapiro, P. R., Iliev, I. T., & Raga, A. C. 2004, MNRAS, 348, 753

Sheth, R. K. & Tormen, G. 2002, MNRAS, 329, 61

Shull, J. M., & van Steenberg, M. E. 1985, ApJ, 298, 268

Sokasian, A., Yoshida, N., Abel, T., Hernquist, L., & Springel, V. 2004, MNRAS, 350, 47

Spergel, D. N., et al. 2003, ApJS, 148, 175

Tegmark, M., Silk, J., Rees, M. J., Blanchard, A., Abel, T., & Palla, F. 1997, ApJ, 474, 1

Whalen, D., Abel, T., & Norman, M. L. 2004, ApJ, 610, 14

White, R. L., Becker, R. H., Fan, X., & Strauss, M. A. 2003, AJ, 126, 1

Wise, J. H., & Abel, T. 2005, ApJ, 629, 615

Yoshida, N., Abel, T., Hernquist, L., & Sugiyama, N. 2003, ApJ, 592, 645

## A. Star Formation in Haloes

Consider a halo of mass  $M$  at time  $t$ . The average number of smaller halos with mass between  $M'$  and  $M' + dM'$  at  $t' < t$  that are located within the halo of mass  $M$  at  $t$  is given by the extended PS formalism,

$$N_{LC}(M', t' \rightarrow M, t) dM' = \frac{M}{M'} \frac{df(M', t' | M, t)}{dM'} dM', \quad (A1)$$

where  $df/dM'$  is the conditional probability for a mass element to be part of a halo of mass  $M'$  at  $t'$ , given that it is part of a larger halo of mass  $M > M'$  at a later time  $t > t'$  (eq. [2.16] in Lacey & Cole 1994). The rate at which stars form at  $t'$  in halos of mass between  $M'$  and  $M' + dM'$ , which will be found within the halo of mass  $M$  at  $t$ , is

$$\frac{dN_{\star}(M', t' \rightarrow M, t)}{dt'} dM' = N_{LC}(M', t' \rightarrow M, t) dM' \frac{dP_{\star}(M', t')}{dt'}, \quad (\text{A2})$$

where  $dP_{\star}(M', t')/dt'$  is the probability per unit of time that a halo with mass  $M'$  forms a star at  $t'$ .

This latter probability is obtained by noting that the probability for a star to form in a halo with mass  $M'$  between  $t'$  and  $t' + dt'$  is equal to the probability for the corresponding halo to form between  $t_f$  and  $t_f + dt_f$ , being  $t_f(M', t') - t'$  the required cooling time in this halo to form a star at  $t'$ , times the probability  $P_{\star}^{\text{first}}(M', t')$  that no halo ancestor has previously formed any star,

$$\frac{dP_{\star}(M', t')}{dt'} dt' = P_{\star}^{\text{first}}(M', t') \frac{dP(M', t', t_f)}{dt_f} dt_f. \quad (\text{A3})$$

In equation (A3),  $dP(M', t', t_f)/dt_f$  is the probability distribution function of halo formation times  $t_f$ , and the derivative  $dt_f/dt'$  is to be evaluated by requiring the condition  $t' = t_f + t_{\text{cool}}(M', t')$ . Although a better behaved definition of halo formation time with known analytical expressions of the corresponding probability distribution function can be found in the literature (Raig et al. 2001), for simplicity we use here that provided by Lacey & Cole (1993). These authors define the formation time of a halo with mass  $M$  at  $t$  as the earliest time  $t_f < t$  at which some progenitor reaches a mass  $M' \geq M/2$ .

At the same time, the average number of stars that have previously formed in ancestors of the halo with mass  $M$  at  $t$ ,  $N_{\star}(M, t)$ , is obtained by integration of equation (A2),

$$N_{\star}(M, t) = \int_0^t dt' \int_0^M dM' N_{LC}(M', t' \rightarrow M, t) \frac{dP_{\star}}{dt'}[M', t']. \quad (\text{A4})$$

Assuming a Poisson distribution of the number of metal-free stars formed in ancestors of a halo of mass  $M$  at  $t$ , with mean expectation value provided by equation (A4), the probability that no ancestor has previously formed any metal-free star is

$$P_{\star}^{\text{first}}(M, t) = e^{-N_{\star}(M, t)}. \quad (\text{A5})$$

Notice that in order to calculate the previous probability we must proceed in an iterative way since the term  $dP_{\star}/dt'$  in equation (A4) includes the factor  $P_{\star}^{\text{first}}(M', t')$  affecting its ancestors, implying that we need to save at each step the information of all previous halos along the merger tree.

Another useful quantity is the metal-free cosmic star formation rate,  $dN_\star/dt$ . This is readily obtained from  $dp_\star/dt$  (eq. [A3]) by integrating over all masses with the halo mass function  $N_h(M, t)$

$$\dot{N}_\star(t) = \int_0^\infty dM N_h(M, t) \frac{dP_\star[M, t]}{dt}. \quad (\text{A6})$$

Table 3. Electron scattering optical depth to the CMB,  $\tau_e$ , obtained for the different metal-free stellar masses and feedback effects considered in this work.

Model	X-rays ( $E_X$ )			
	No feed.		Diss.	$10^{51}$ erg
	A	B	C	D
1	0.084	0.077	0.066	0.057
2	0.116	0.103	0.087	0.068
3	0.094	0.089	0.079	0.066
4	0.121	0.110	0.096	0.076
5	0.105	0.102	0.094	0.082
6	0.127	0.119	0.108	0.090

Table 4. Total number of photons emitted per baryon by metal-free stars obtained for the different metal-free stellar masses and feedback effects considered in this work.

Model	X-rays ( $E_X$ )			
	No feed.		Diss.	$10^{51}$ erg
	A	B	C	D
1	0.46	0.33	0.18	0.07
2	0.80	0.61	0.40	0.19
3	0.39	0.29	0.16	0.06
4	0.73	0.56	0.38	0.18
5	0.31	0.24	0.14	0.06
6	0.62	0.49	0.34	0.16